Study of transition metal aluminide alloys

1997 J. Phys.: Condens. Matter 9 3529

(http://iopscience.iop.org/0953-8984/9/17/004)

J. Phys.: Condens. Matter **9** (1997) 3529–3541. Printed in the UK PII: S0953-8984(97)76881-4

Study of transition metal aluminide alloys

Indra Dasgupta†§, Tanusri Saha-Dasgupta†‖, Abhijit Mookerjee†¶ and Gour Prasad Das‡+

† SN Bose National Centre for Basic Sciences, JD Block, Sector 3, Salt Lake City, Calcutta 700091, India

‡ Solid State Division, Bhabha Atomic Research Centre, Trombay, Mumbai 500010, India

Received 2 August 1996, in final form 30 December 1996

Abstract. We have studied the densities of states of the series of alloys FeAl, CoAl, and NiAl, each in the disordered state, using the augmented-space recursion technique coupled with the tight-binding muffin-tin orbitals method. We have estimated the local moments in these alloys using the spin-polarized version of the tight-binding linearized muffin-tin orbitals method. We have also obtained the effective pair interactions for these alloys.

1. Introduction

The aluminides of the transition metals Fe, Co, and Ni form a very interesting series as regards the study of electronic properties. There is strong p–d hybridization between the p states of Al and the d states of the transition metals. The d band becomes systematically filled up as we go up the series from Fe to Ni, and the strong hybridization with Al results in the filling up of the unfilled d band of the transition metal. A very important factor, which motivates the study of this alloy series, is the fact that at around the 50% composition all three of the aluminides have the same underlying bcc crystalline structure. In the ordered state, all three are in the B2 atomic configuration. This means that any trend in behaviour among the members in the series arises principally due to their electronic properties. A systematic study of the ordered alloys has been recently carried out in the framework of the tight-binding linearized muffin-tin orbitals (TB-LMTO) technique [1], as well as in the linearized augmented-plane-wave (LAPW) method [2], and the full-potential LAPW method [3]. In the present communication we shall study the effect of disorder on the alloy series, specifically studying the pair potentials, and consequently the phase stability and ordering energies, as well the effect on the density of states at the Fermi level after alloying.

Recent advances in the first-principles theories of metals and alloys are based on the local density approximation in the framework of the density functional theory (LDA). The calculations of the ground-state properties of materials based on the LDA have been shown to produce results of metallurgical accuracies. For the ordered intermetallics with underlying periodicity, the equations based on the LDA can be solved to a high degree of precision using standard band theory techniques like the Korringa–Kohn–Rostoker (KKR), the LAPW,

§ Present address: Max-Planck-Institut für Festkörperforschung, Heisenberger Straße 1, Stuttgart, Germany; e-mail: dasgupta@radix7.mpi-stuttgart.mpg.de.

‖ Present address: ONERA, BP 72, 92322 Châtillon Cédex, France; e-mail: dasgupta@onera.fr.

¶ E-mail: abhijit@bose.ernet.in.

+ E-mail: gpd@magnum.barct1.ernet.in.

0953-8984/97/173529+13$19.50

and the linearized muffin-tin orbitals (LMTO) methods. However, for the disordered alloys, the absence of translational symmetry inhibits the use of usual band-structure methods for disordered alloys. In addition, to calculate any quantity one has to perform configuration averaging over all realizations of the random variables characterizing the Hamiltonian. The most common method of treating disorder is that of using the coherent potential approximation (CPA), which is a mean-field approximation in which the homogeneity of the disorder restores the translational symmetry in the averaged quantities. The main disadvantage of the CPA is that it is a single-site approximation, and therefore has its own limitations. In particular it cannot be extended to take into account local clustering and short-ranged ordering tendencies, or the effects of local lattice distortions due to large degrees of size mismatch between the constituents of the alloy.

Recently there have been attempts to take into account the off-diagonal disorder effect in disordered NiAl alloy within the single-site CPA framework following the method of Blackman, Esterling and Berk (BEB) [4]. We have recently proposed a method based on the real-space recursion and augmented-space formalism in the framework of the TB-LMTO technique for the description of the electronic structure of random alloys [5]. Within this formalism, one constructs a non-random Hamiltonian defined on a new Hilbert space which is a direct product of the Hilbert space spanned by the original Hamiltonian basis and a configuration space spanned by the various allowed configuration states of the disordered Hamiltonian. The augmented-space theorem [6] then relates the average of any function of the Hamiltonian to a matrix element on a particular subspace of the augmented space. This configuration averaging in the augmented space is *exact*, and its coupling with the recursion method [7] allows configuration fluctuation effects of reasonably large clusters to be taken into account, and it does not involve any single-site approximation such as the CPA, and treats diagonal and off-diagonal disorder *on an equal footing*. The aim of the present communication is to use the augmented-space recursion (ASR) in conjunction with the TB-LMTO technique to study the electronic structure of transition metal aluminides.

The remainder of the paper is organized as follows. In section 2 we shall very briefly present our methodology for the determination of the densities of states and effective pair interactions. Section 3 will deal with the densities of states, the study of the effective pair interactions, and the ordering energies. In section 4 we will present our conclusions.

2. Methodology

2.1. The density of states

The basis of our calculations will be the tight-binding linearized muffin-tin orbitals formalism introduced by Andersen and co-workers [8, 9], coupled with the augmented-space method [6, 10–12], and the recursion method [7, 13]. All of these techniques have been described extensively earlier, and readers are referred to the above references for technical details.

The calculation of the electronic density of states in random systems essentially involves the determination of the averaged resolvent or the Green operator. According to the augmented-space theorem [6], the configuration-averaged resolvent is given by

$$\langle G(E)\rangle = \langle \nu^0|(E\tilde{I} - \tilde{H})^{-1}|\nu^0\rangle$$

where $\tilde{H}$ is the Hamiltonian defined in the extended augmented space involving both the original Hilbert space spanned by the TB-LMTO basis and the configuration space. For binary alloys, the configuration space is isomorphic to the configuration space of a spin-1/2

Ising model (with binary states labelled ↑ and ↓ at each site). The state $|\nu^0\rangle$ corresponds to the state with ↑ at each site.

The TB-LMTO Hamiltonian in its most localized form, generalized to random alloys, is given by

$$H^{\alpha(\text{alloy})}_{RL,R'L'} = \hat{C}^{\alpha}_{RL}\delta_{RR'}\delta_{LL'} + (\hat{\Delta}^{\alpha})^{1/2}_{RL} S^{\alpha}_{RL,R'L'} (\hat{\Delta}^{\alpha})^{1/2}_{R'L'} \tag{1}$$

where $\hat{C}_{RL} = C^A_{RL} n_R + C^B(1 - n_R)$; $\hat{\Delta}^{1/2}_{RL} = (\Delta^A_{RL})^{1/2} n_R + (\Delta^B_{RL})^{1/2}(1 - n_R)$, C^A_{RL}, C^B_{RL}, Δ^A_{RL}, and Δ^B_{RL} are the potential parameters of the constituents A and B of the alloy, and n_R are local site-occupation variables which randomly take the values 1 or 0 according to whether the site is occupied by an A atom or not, with probabilities proportional to the concentrations of the constituents. According to the prescription of the augmented-space formalism, the effective non-random Hamiltonian in augmented space is then constructed from the random Hamiltonian $H^{\alpha(\text{alloy})}_{RL,R'L'}$ by replacing the random variable $\{n_R\}$ by corresponding self-adjoint operators $\{\tilde{M}_R\}$, whose representations are given by

$$I \otimes I \otimes \cdots \otimes M_R \otimes \cdots$$

$$M_R = x_A|\uparrow_R\rangle\langle\uparrow_R| + x_B|\downarrow_R\rangle\langle\downarrow_R| + \sqrt{x_A x_B}\,\{|\uparrow_R\rangle\langle\downarrow_R| + |\downarrow_R\rangle\langle\uparrow_R|\}$$

where x_A and x_B are the concentrations of the A and B constituents. Once the effective Hamiltonian has been set up, the recursion method provides an algorithm for calculating diagonal matrix element of the resolvent or Green function associated with the effective Hamiltonian $\tilde{H}$.

The fact that the configuration space of the occupation variables is isomorphic to the spin-1/2 Ising model can be exploited in the development of stable and efficient computer codes employing the multi-spin coding technique of Ising computational methodology. We have further reduced the rank of the invariant subspace on which the recursion operates by utilizing the point group symmetries of the augmented space arising out of the homogeneity of the disorder and [10–12]. In order to reduce the amount of computer storage necessary one can make further use of the point group symmetry in the augmented space arising out of the homogeneity of the disorder. All of these facts have been discussed in great detail in previous communications referred to earlier.

2.2. The effective pair interaction and orbital peeling

Studies of phase stability, starting from the disordered side, usually begin with setting up local concentration fluctuations in a completely disordered medium, and expansion of the change in configurational energy in terms of effective multi-site interaction energies [14, 15]. For stability studies the dominant role is played by the effective pair interaction energies (EPI). These are formally defined as

$$E_{pq} = V_{AA} + V_{BB} - V_{AB} - V_{BA}$$

where V_{IJ} is the total average energy with atomic species I and J at sites p and q respectively. The EPI can be further expressed in a convenient form, in terms of the generalized phase shift $h(E)$, as

$$E_{pq} = -\int_{\infty}^{E_F} \operatorname{Im} h(E)\, \mathrm{d}E$$

with

$$h(E) = (1/\pi) \log\det \frac{\langle G^{AA}\rangle\langle G^{BB}\rangle}{\langle G^{AB}\rangle\langle G^{BA}\rangle}$$

where $\langle G^{AA}\rangle$, $\langle G^{BB}\rangle$, $\langle G^{AB}\rangle$, and $\langle G^{BA}\rangle$ describe the Green functions with two atoms in all possible combinations embedded in positions p and q. The operation involved in the definition of the EPI is an exchange of the atoms on sites p and q. Since the sub-block of the effective Hamiltonian $\tilde{H}$ relative to all atoms except those at sites p and q is unaltered under this exchange, *the orbital peeling method* [16] provides an efficient means of obtaining generalized phase shifts. The central result of the application of the orbital peeling method is the effective pair interaction expressed in terms of zeros and poles of the resolvent $\langle G^b_{IJ}\rangle$, where $\langle G^b_{IJ}\rangle$ is the averaged Green function corresponding to the effective Hamiltonian, where two atoms are embedded at sites I and J, in which the orbitals from 1 to $b-1$ are deleted at the site I. Thus the whole process reduces to determining the configuration-averaged Green function $\langle G^b_{IJ}\rangle$. We can do this by using the ASR [5], and the resulting coefficients are used to estimate the positions of the zeros and poles required in the orbital peeling result. Notice that, by definition, the EPI are small quantities ($\simeq$O(mRyd) formed by differences of relatively large energies ($\simeq$O(Ryd)). Instead of calculating the large quantities and then taking their differences, thus causing large errors, we obtain this difference directly by orbital peeling.

3. Results and discussion

3.1. Computational details

Before we discuss our results, we should mention some details of the calculation procedure. The total energy density functional calculations were performed for the ordered aluminides in the B2 structure for the 50% compounds with their equilibrium lattice constants. The density-of-states calculations were performed within the TB-LMTO method in the atomic sphere approximation, and the calculations were done semi-relativistically (i.e. using the scalar relativistic correction). The exchange–correlation potential of von Barth and Hedin was used. The basis set was composed of $l = 0, 1, 2$ orbitals, so the Hamiltonian matrix elements were of rank 9. The self-consistent potential parameters for the ordered alloys in the B2 structure were used to parametrize the random bcc alloys. These are shown in table 1.

To parametrize the random-alloy Hamiltonian we tried out two procedures. In the first, the self-consistent potential parameters for the B2 ordered alloys were used for random bcc alloys as well. It has sometimes been assumed that on doing this a major part of the charge transfer on alloying is already taken into account. Disorder will certainly affect the charge transfer, but that effect is assumed to be small. Thus a further (LDA) self-consistency loop is assumed not to be necessary. In the second procedure we carried out the full ASR-LDA self-consistency procedure to examine whether such an assumption is valid or not. Both of the calculations were carried out for the experimental value of the lattice constant. The self-consistent ASR potential parameters are shown for comparison in the right-hand columns of table 1. The following scenario may be presented: in the ordered case, each transition metal is surrounded by eight Al atoms, whereas, in the 50–50 disordered alloy, each transition metal atom is effectively surrounded by four transition metal and four Al atoms on average. The charge-transfer effects may be quite different. This fact is reflected in the calculated properties, to be discussed later in the text. In particular, we note that the effect on the density of states is small apart from a rigid shift; however, the effect on the stability characteristics is significant. We conclude that full ASR-LDA self-consistency is essential for studying phase stability.

The treatment of Madelung energy in a disordered alloy is always a problem. Many

Table 1. Top: the converged potential parameters for NiAl, CoAl, and FeAl in the B2 structures for the 50–50 concentration. The calculations were done with the combined corrections turned off. Bottom: the converged potential parameters for disordered NiAl, CoAl, and FeAl for the 50–50 concentration. The calculations were done using ASR.

Aluminides in the B2 structure								
	NiAl							
	Ni				Al			
l	E_v	C	Δ	γ	E_v	C	Δ	γ
0	−0.4656	−0.3405	0.1802	0.4257	−0.5344	−0.5306	0.1611	0.4162
1	−0.3018	0.6750	0.1680	0.1130	−0.3007	0.3621	0.1401	0.1048
2	−0.1742	−0.1402	0.0119	−0.0036	−0.2116	1.5917	0.1401	0.0533
	CoAl							
	Co				Al			
l	E_v	C	Δ	γ	E_v	C	Δ	γ
0	−0.4622	−0.2749	0.1926	0.4293	−0.5161	−0.5114	0.1672	0.4169
1	−0.2828	0.7730	0.1770	0.1146	−0.2799	0.3995	0.1448	0.1051
2	−0.1370	−0.0782	0.0145	−0.0017	−0.1698	1.6373	0.1427	0.0536
	FeAl							
	Fe				Al			
l	E_v	C	Δ	γ	E_v	C	Δ	γ
0	−0.4463	−0.2343	0.1945	0.4312	−0.5067	−0.5168	0.1635	0.4161
1	−0.2864	0.8070	0.1795	0.1160	−0.2656	0.3794	0.1415	0.1046
2	−0.1269	−0.0460	0.0163	0.0002	−0.1591	1.6041	0.1401	0.0535
Disordered aluminides								
	NiAl							
	Ni				Al			
l	E_v	C	Δ	γ	E_v	C	Δ	γ
0	−0.3728	−0.2797	0.2081	0.4273	−0.4703	−0.5229	0.1338	0.4108
1	−0.2576	0.8532	0.1906	0.1141	−0.2603	0.2652	0.1175	0.1028
2	−0.1840	−0.1503	0.0139	−0.0025	−0.1410	1.3949	0.1219	0.0535
	CoAl							
	Co				Al			
l	E_v	C	Δ	γ	E_v	C	Δ	γ
0	−0.3418	−0.2085	0.2142	0.4298	−0.4684	−0.5126	0.1405	0.4122
1	−0.2355	0.9299	0.1956	0.1156	−0.2390	0.2972	0.1226	0.1030
2	−0.1280	−0.0710	0.0163	−0.0010	−0.1200	1.4451	0.1255	0.0534
	FeAl							
	Fe				Al			
l	E_v	C	Δ	γ	E_v	C	Δ	γ
0	−0.3025	−0.1705	0.2087	0.4308	−0.4590	−0.5176	0.1392	0.4114
1	−0.2133	0.9293	0.1906	0.1165	−0.2072	0.2860	0.1207	0.1021
2	−0.1049	−0.0238	0.0175	−0.0007	−0.1417	1.4353	0.1253	0.0536

authors neglect it entirely. We adopt here a procedure suggested by Drchal *et al* [17]: that of choosing unequal AS radii around the transition metal and Al atoms such that the atomic spheres have almost zero excess charge, but conserve the total charge. However, we were careful that such a choice does not violate the overlap criterion of Andersen and Jepsen [9]. In the ASR-LDA self-consistency loop, charge transfer takes place between these spheres; however, at the end of the self-consistent iterations, the spheres are approximately neutral, and hence do not contribute a Madelung term to the energy. This prescription is quite *ad hoc*, and there is no guarantee in general that we will be able to find such AS radii. In fact, in systems where ionic bonding dominates, such a procedure is sure to prove unsuccessful. This is a weak point in our treatment. Recently, an alternative method has been suggested in connection with the CPA by Korzhavyi *et al* [18]. They went beyond the conventional single-site averaging of the CPA to include correlated charge-fluctuation effects in the Madelung energy. We believe that the method suggested is superior to the one adopted here. However, we have not implemented a generalization of this method to the ASR in this communication.

For the purposes of augmented-space recursion, a real-space map of 400 atoms was used to generate the augmented-space cluster. The rank of this space was then drastically reduced using the point group symmetries of the underlying lattice, the symmetries of the configuration space, because of the homogeneity of the disorder†, and the symmetries of the starting state. This is possible because of the fact that recursion, which begins from a state in a given irreducible subspace of the full augmented space, *cannot* mix states of different irreducible subspaces and is effectively confined within the subspace to which the starting state belongs [13]. The reduction procedure and the generation of the weighted recursion have been described in detail in an earlier communication [5]. The recursion was carried out up to eight steps, and then supplemented with the analytic terminator of Lucini and Nex [19].

Table 2. Electronic characteristics of ordered alloys.

	FeAl	CoAl	NiAl
$E_{\text{non-bonding}} - E_F$	0.06	0.11	0.16
$E_{\text{bonding}} - E_F$	−0.25	−0.30	−0.30
$E_{\text{anti-bonding}} - E_F$	0.10	−0.013	−0.04
$n(E_F)$	9.0175	2.1730	2.8725
Charge transfer	0.277	0.336	0.417

3.2. The electronic density of states for ordered and disordered alloys

The results of our ordered self-consistent scalar relativistic LMTO-ASA calculation (without the combined correction) is presented in figure 1 for NiAl, CoAl, and FeAl. The relevant quantities obtained from the density of states are shown in table 2.

The density of states possesses sharp features typical of ordered compounds. The main features of the density of states around the Fermi energy in all of the aluminides arise from the transition metal sites, since the aluminium-site sp contribution is relatively flat and

† For example, all eight different configurations with an Fe atom at the centre and seven Al atoms and one Fe atom at the bcc nearest-neighbour positions are exactly equivalent, with the same weight.

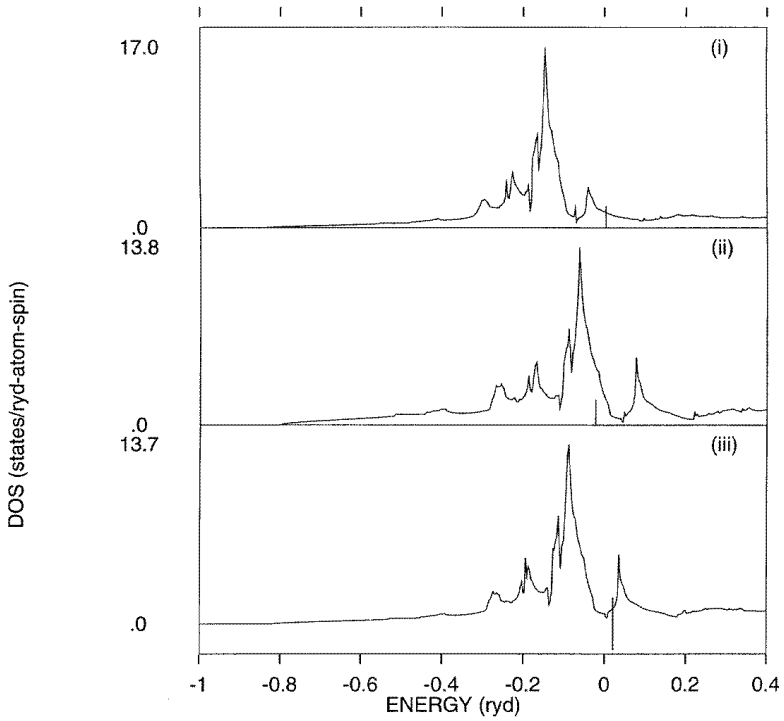

Figure 1. Densities of states for the ordered aluminides (i) NiAl, (ii) CoAl, and (iii) FeAl. The Fermi levels are marked with vertical lines.

featureless. The prominent feature is the presence of large non-bonding peaks at energies of -0.1228 Ryd, -0.0653 Ryd, and 0.0664 Ryd for NiAl, CoAl, and FeAl, respectively, and satellite bonding and anti-bonding peaks, on either side of the non-bonding peak. It is observed as we move from NiAl to FeAl that the weight from the non-bonding peak gets transferred to the bonding and anti-bonding peaks. As a result, the bonding and anti-bonding peaks for FeAl are more prominent as compared to those for NiAl. From figure 1 we find that: for FeAl, the Fermi energy lies in the steeply falling part of the non-bonding peak; while for CoAl, the Fermi energy falls almost in the pseudo-gap between the non-bonding and anti-bonding peaks, leading to a small value of the density of states at the Fermi energy. For NiAl, as the number of electrons available to fill the band increases still further, the Fermi energy falls in the non-bonding peak. This leads to a non-monotonic behaviour of the density of states at the Fermi level as we go from Fe to Ni–Al. The XPS studies by Fuggle *et al* [20] confirm this picture of band filling in the aluminide series.

Figure 2 shows the density of states for the disordered alloys. These are obtained from the self-consistent ASR potential parameters. Table 3 gives details of the differences between the results of these calculations and those obtained from ordered B2 potential parameters. A detailed comparison of the structures observed in the densities of states is given in the first four rows of table 3. As expected, the difference in charge transfer due to different local environments in the B2 and disordered structures leads to an almost rigid shift in the peak positions.

There are two prominent peaks in the density of states which may be identified (by comparison with figure 1) as the bonding and the non-bonding peaks. The anti-bonding

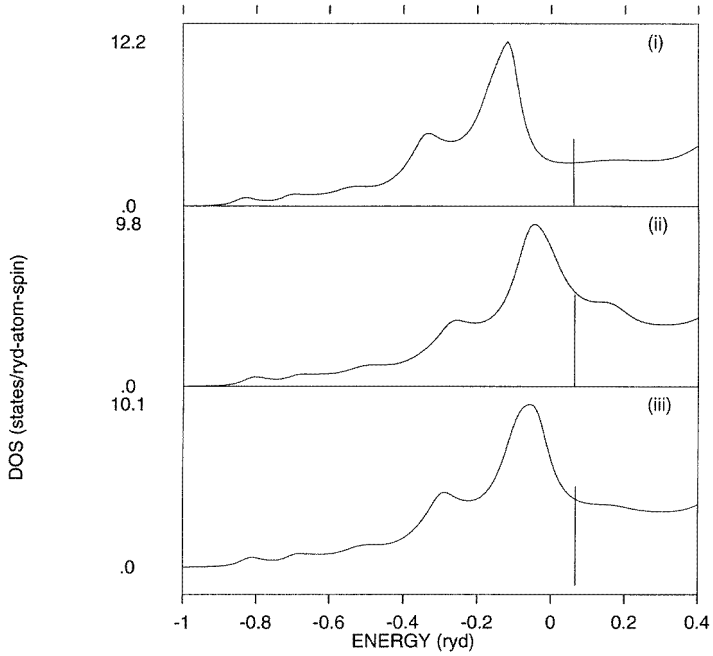

(a)

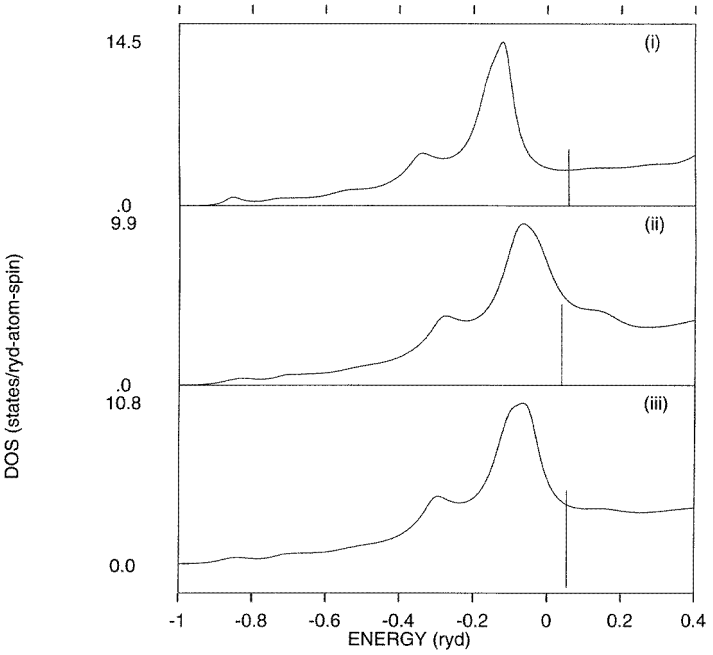

(b)

Figure 2. Densities of states for the disordered aluminides parametrized by LDA self-consistent ASR potential parameters: (i) NiAl, (ii) CoAl, and (iii) FeAl. (a) Non-self-consistent ASR and (b) self-consistent ASR. The Fermi levels are marked with vertical lines.

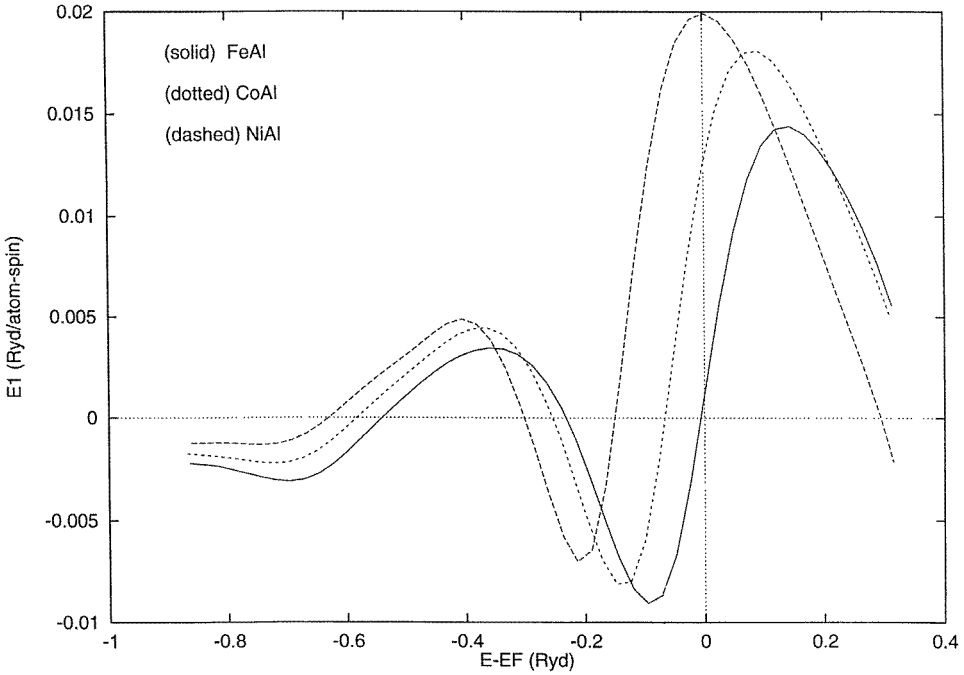

Figure 3. Nearest-neighbour effective pair interactions plotted as functions of $E - E_F$ for the alloys NiAl, CoAl, and FeAl.

peak is mostly suppressed by disorder broadening, and becomes prominent only for FeAl. The two-peaked nature of the density of states of NiAl is in agreement with the KKR-CPA results [21] as well as the TB-LMTO-CPA results, but it does not agree with the results obtained by TB-LMTO method coupled with BEB method [4]. The CPA results do not show any trace of the anti-bonding peak in any of the aluminides. The ratio of the heights of the lower-energy peak (presumably the bonding peak) and the higher-energy peak (presumably the non-bonding peak) is around 0.7 to 0.8 in the aluminide series. In the ASR calculations, apart from those for NiAl, there are 'reminders' of the anti-bonding peaks for both FeAl and CoAl. Moreover the bonding and the non-bonding peaks are better resolved, with the height ratios varying between 0.5 and 0.6. It is known from earlier work using the ASR (which goes beyond the single-site approximation of the CPA and takes into account effects of configuration fluctuations in clusters) that there is always a better resolution of bonding–anti-bonding and non-bonding structures in the density of states as compared with the case for the single-site CPA. These structures arise from pairs, and begin to show up in two-site CPAs [22].

The position of the Fermi energy, though shifted, has a similar trend to that for ordered compounds. Interestingly, the value of $n(E)$ follows the systematic trend observed experimentally for Pauli paramagnetic susceptibility. This may be attributed to the fact that disorder fills up the pseudo-gap between the anti-bonding and non-bonding states, $(E_{\mathrm{anti-bonding}} - E_{\mathrm{non-bonding}})$, for the CoAl, resulting in a sharp increase in the density of states at E_F, compatible with experimental observations. We also find, analogously to the case for the ordered densities of states, that the weight from the non-bonding peak gets transferred to the bonding and anti-bonding peaks as we move from NiAl to FeAl.

Table 3.

	Self-consistent			Non-self-consistent		
	FeAl	CoAl	NiAl	FeAl	CoAl	NiAl
E_F[a]	0.0554	0.0609	0.0567	0.0320	0.0480	0.0519
$E_B - E_F$[b]	0.3132	0.3523	0.3932	0.3070	0.3420	0.3878
$E_N - E_F$[c]	0.0990	0.1162	0.1739	0.0980	0.1132	0.1747
$E_A - E_F$[d]	0.0860	0.0970	†	0.1240	0.0920	†
$n(E_F)$[e]	5.876	4.299	3.205	5.876	4.087	3.167
E_1[f]	1.16	12.78	19.92 12.50‡ 9.50§	−8.25	1.45	9.25
E_2	−2.03	0.18	0.87	−2.30	10^{-4}	0.98
E_3	0.424	0.446	0.370	−0.204	−0.390	−0.592
E_4	−0.071	−0.119	−0.136	−0.048	−0.094	−0.1773
E_5	−0.093	−0.0003	0.268	0.2275	0.1651	0.462
E_{ord}[g]	−2.0433	−11.97	−18.71 −10.15‡	No Order	−2.045	−9.40
(Experiment)	Ordered	Ordered	Ordered			
$\boldsymbol{k}_{min}$[h]	(100)	(100)	(100)	(000)	(100)	(100)
$V(\boldsymbol{k}_{min})$	−15.4	−92.0	−144.0	—	−13.81	−70.11
T_0 (K)[i]	1183	7305	113 85			

[a] The Fermi energy in Ryd.
[b] The bonding peak position measured from the Fermi energy in Ryd.
[c] The non-bonding peak position measured from the Fermi energy in Ryd.
[d] The anti-bonding peak position measured from the Fermi energy in Ryd.
[e] The density of states at the Fermi energy in states Ryd^{-1}/(atom spin).
[f] Pair energies in mRyd/(atom spin).
[g] The ordering energy in mRyd/(atom spin).
[h] $\boldsymbol{k}$ at which $V(\boldsymbol{k})$ has a minimum. If this is (000) that indicates phase separation; if not it indicates ordering of the type specified by $\boldsymbol{k}_{min}$.
[i] The order–disorder transition temperature in K.
† For NiAl the anti-bonding peak is hardly discernible.
‡ These are KKR-CPA calculations.
§ These are BEB calculations [4].

3.3. Effective pair interactions and phase stability

As mentioned in the introduction, at zero temperature all of the three alloys NiAl, CoAl, and FeAl occur in the B2 phase. Among these B2 alloys, CoAl and NiAl are known to be strongly ordered, and are deformed by an anomalous ⟨100⟩ slip plane (in contrast to the ⟨111⟩ slip plane for the bcc-based materials), while FeAl is weakly ordered and is known to be relatively ductile (and has ⟨111⟩ slip planes). In the present section we will present our

calculations for the phase stability of these alloys. Again our calculations were done with potential parameters obtained from self-consistent ordered calculations for the B2 phase, as well as self-consistent ASR calculations. The various results are compared in table 3.

We have calculated the effective pair interactions for the three alloys NiAl, CoAl, and FeAl up to the fifth-nearest neighbours (E_1 to E_5). The more distant pairwise interactions are neglected. In figure 3 we have shown E_1 for the three alloys as a function of $E - E_F$ obtained from self-consistent ASR calculations. We find that the nature of E_1 as a function of energy is the same for all three alloys, apart from a rigid shift. We also note that the value of E_1 at E_F decreases as we move from NiAl to FeAl, suggesting that FeAl is relatively weakly ordered.

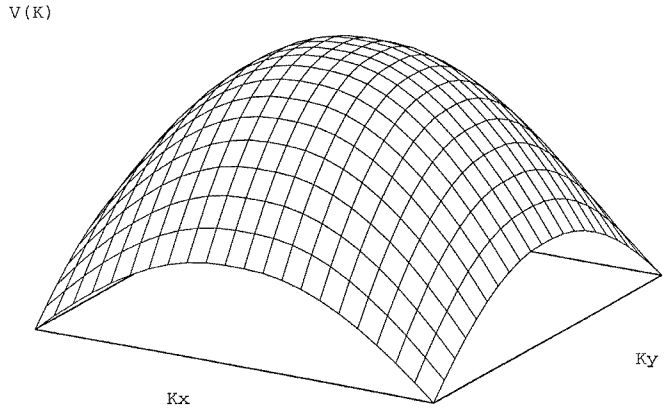

(a)

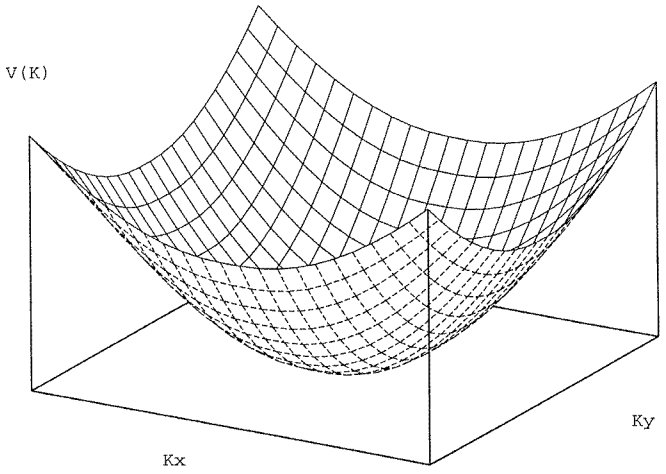

(b)

Figure 4. (a) $V(\boldsymbol{k})$ at $k_z = 0$ for FeAl for the self-consistent ASR. (b) The same, but for B2 parameters.

We note from table 3 that the results are very different for the calculations with potential parameters obtained from B2 calculations, and those with potential parameters obtained from self-consistent ASR calculations. The effect of charge transfer is in both cases manifested

as a rigid shift. However, this rigid shift in the case of self-consistent ASR calculations is such that we obtain correct ordering tendencies in the alloys. For FeAl, in particular, the self-consistent ASR calculations show that $E_1 > 0$, and

$$V(\boldsymbol{k}) = \sum_{\boldsymbol{R}} (\exp \mathrm{i}\boldsymbol{k} \cdot \boldsymbol{R}) E_n$$

has a minimum at the correct special point, namely the X point (figure 4(a)). However, the calculations with the B2 potential parameters show that, for FeAl, $E_1 < 0$, and $V(\boldsymbol{k})$ has a minimum at the Γ point (figure 4(b)). This indicates a phase segregation tendency in FeAl, which is certainly wrong. This shows that LDA self-consistency in the disordered phase is essential for phase stability studies.

Below we discuss some of our results obtained from self-consistent ASR calculations.

The ordering energy for the B2 phase considering up to third-nearest-neighbour interaction is given by [23]

$$E^{ord} \simeq -E_1 + (3/4)E_2 + (3/2)E_3.$$

Our calculated value of E^{ord} for NiAl turns out to be -18.71 mRyd/atom which compares reasonably well with the KKR-CPA-GPM [21] value of -10.15 mRyd/atom. The corresponding ordering energy for CoAl alloys is found to be -11.97 mRyd/atom, and that for FeAl only -2.04 mRyd/atom, indicating NiAl and CoAl alloys to be more strongly ordered than FeAl. The mean-field order–disorder transition temperature $T_c = x_A x_B V(k_{min})$ of FeAl turns out to be around 1183 K. The experimental result is quoted as 1341 K. The underestimation of the value may be attributed to the neglect of the more distant nearest-neighbour interactions in the expansion of the configurational energy. Furthermore, triplet and higher-order interactions may not be negligible. The transition temperatures for CoAl and NiAl are 7305 K and 11 385 K respectively. Both of these are higher than the respective melting temperatures. This suggests that both of these are strongly ordered solids.

4. Conclusions

In conclusion, we have presented a systematic study of the densities of states and phase stabilities of the transition metal aluminide series NiAl, CoAl, and FeAl, via fully self-consistent ASR calculations. We have demonstrated that the proper LDA self-consistency is crucial for predicting the ordering tendencies in these alloys. Several earlier studies of the phase stabilities of one or more of the transition metal aluminides (references are given in the text) have been carried out either from the ordered side or using the generalized perturbation method based on the CPA. We view our work as complementary to the earlier work, bringing in ideas from the embedded-cluster method and concentration-wave methods based on the ASR. The conclusions are in agreement with the earlier ones, and until better estimates of the entropy are available, the estimates of the ordering temperatures are reasonable, but perhaps not accurate enough for comparison.

Acknowledgments

We should like to thank the Department of Science and Technology, Government of India, for financial assistance through its project No DST/MEM/M-94. We should also like to thank Professor J Kudrnovský for the use of his TB-LMTO-CPA programs as a starting point for our ASR iterative loops. We also acknowledge several important discussions with him about this work. The work was motivated and begun during the Working Group on Alloy Phase Stability held at ICTP, Trieste, during the summer of 1994.

References

[1] Sundarajan V, Sahu B R, Kanhere D G, Panat P V and Das G P 1995 *J. Phys.: Condens. Matter* **7** 6019
[2] Singh D J 1992 *Phys. Rev.* B **46** 14 392
[3] Fu C L, Ye Y Y, Hoo M H and Ho K M 1995 *Phys. Rev.* B **48** 6712
Zou Z and Fu C L 1995 *Phys. Rev.* B **51** 2115
[4] Sluiter M H F and Singh P P 1984 *Phys. Rev.* B **49** 10 918
[5] Saha T, Dasgupta I and Mookerjee A 1994 *J. Phys.: Condens. Matter* **6** L245
[6] Mookerjee A 1973 *J. Phys. C: Solid State Phys.* **6** 1340
[7] Haydock R, Heine V and Kelly M J 1972 *J. Phys. C: Solid State Phys.* **5** 2845
[8] Andersen O K 1975 *Phys. Rev.* B **12** 3060
[9] Andersen O K and Jepsen O 1984 *Phys. Rev. Lett.* **53** 2571
Andersen O K, Kumar V and Mookerjee A (ed) *Proc. Workshop on Electronic Structure of Metals and Alloys (Trieste)* (Singapore: World Scientific)
[10] Mookerjee A and Prasad R 1993 *Phys. Rev.* B **48** 17 724
[11] Saha T, Dasgupta I and Mookerjee A 1994 *Phys. Rev.* B **50** 13 267
[12] Dasgupta I, Saha T and Mookerjee A 1995 *Phys. Rev.* B **51** 3413
[13] Haydock R 1980 *Solid State Physics* vol 35 (New York: Academic)
[14] Ducastelle F and Gautier F 1976 *J. Phys. F: Met. Phys.* **6** 2039
[15] Gonis A, Stocks G M, Butler W H and Winter H 1984 *Phys. Rev.* B **29** 555
[16] Burke N R 1976 *Surf. Sci.* **58** 349
[17] Drchal V, Kudrnovský J and Weinberger P 1994 *Phys. Rev.* B **50** 7903
[18] Korzhavyi P A, Ruban A V, Abrikosov I A and Skriver H L 1995 *Phys. Rev.* B **51** 5773
[19] Lucini M U and Nex C M M 1987 *J. Phys. C: Solid State Phys.* **20** 3125
[20] Fuggle J C, Hillebrecht F U, Zeller R, Zolmerek Z, Bernett P A and Freiburg C 1983 *Phys. Rev.* B **27** 2145
[21] Turchi P E A, Sluiter M, Pinski F J and Johnson D D 1991 *Alloy Phase Stability and Design* vol 186, ed G M Stocks, D D Pope and A F Giamei (Philadelphia, PA: MRS)
[22] Kumar V, Mookerjee A and Srivastava V K 1982 *J. Phys. C: Solid State Phys.* **15** 1939
[23] Turchi P E A 1984 *PhD Thesis* University Pierre et Marie Curie, Paris VI